# Remote sensing of a transboundary Chinese reservoir cascade and its influence on Lai Chau reservoir in the upper Da river basin

Nguyen Tien Quang[1,2], Truong Van Anh[2*], Ngo Le An[1], Hoang Van Dai[3]

**Abstract:** Satellite-based monitoring of reservoir operations in transboundary, data-scarce basins remains a major challenge due to limited in situ observations and restricted data sharing. This study develops an end-to-end workflow on Google Earth Engine to monitor a cascade of nine Chinese reservoirs in the upper Da River and assess their influence on Viet Nam's downstream Lai Chau reservoir. DEM-derived area–elevation–volume curves are generated from NASADEM and reservoir polygons, while a fast Sentinel-1 OtsuSmart classifier produces 7-day water-surface area series that are converted to water level and storage. Validation against survey curves for Lai Chau and Huoi Quang yields r = 1.00, with RMSE values of 1.86 and 0.23 km², respectively, while reconstructed Lai Chau water levels achieve r ≈ 0.80 and RMSE ≈ 5.6 m. Cascade and regulation indices along the Jupudu–Gelantan–Tukahe–Lai Chau chain show that Chinese operations exert first-order control on Lai Chau's seasonal water-level regime, with positive correlations and 0–2-month lags at the monthly scale, while most net dry-season release originates from upstream branches. Daily lag-correlation analysis further reveals tight synchrony between Gelantan and Tukahe but a compensating, one-week out-of-phase response at Lai Chau, indicating active buffering. The framework uses only global open data and is transferable to other transboundary basins.

**Keywords:** Transboundary river, sentinel-1, storage dynamics, Da river basin.

## 1. Introduction

International rivers cross political borders and link riparian states through resource development, regional cooperation, environmental change and geopolitical interests (He et al., 2017). As a result, management problems in these basins are highly complex and sensitive, and difficult to analyse at the scale of the whole watershed. Effective data sharing is a basic prerequisite for transboundary cooperation (Giuliani & Castelletti, 2013), yet in many basins-particularly in developing countries-competition over water use and incomplete or missing hydrological records undermine information exchange and the resolution of disputes (Oliver Olsson, 2010). At the same time, the rapid expansion of large hydropower schemes, including cascades of multipurpose reservoirs in the Greater Mekong and Red River systems, has substantially modified natural flow regimes, while limited disclosure of design parameters and operating rules continues to restrict assessments of past and future impacts and to hinder coordinated basin-wide management (Du et al., 2022).

Remote sensing provides timely, spatially detailed information and is now widely used in environmental monitoring, agriculture, natural resource management, disaster risk assessment and land-related applications…. Recent advances have enabled the reconstruction of reservoir storage dynamics from global satellite products: high-resolution DEMs, optical imagery and radar altimetry have been used to derive elevation–area–storage curves and multi-year storage time series for large reservoirs and cascades and model-based studies have begun to assimilate these products to constrain hydrological simulations and improve reservoir representation in large-scale models (Vu, Dang, Galelli, & Hossain, 2022). End-to-end GEE workflows have mapped inundation from Landsat water indices and converted area to storage (Condeça, Nascimento, & Barreiras, 2022), while tools such as RAT operationalize GEE-derived water extent and area–elevation information to track storage change (Kumar Biswas & Hossain, 2022). In highly regulated Southeast Asian basins, (Du et al., 2022) derived maximum reservoir extents from JRC Global Surface Water, built DEM-based AEV curves (SRTM), and generated area time series using an Edge–Otsu approach; related Vietnam studies combine SAR/optical water mapping (Refined Lee + Otsu) with altimetry or in situ levels to support cross-sensor validation and uncertainty assessment (Cường, 2025; Pham-Duc et al., 2022). However, the upper Da River basin-a key transboundary tributary of the Red River—has received comparatively little attention. Existing work has mainly derived area–elevation curves and analysed water surface area and water-level variations for a subset of Chinese reservoirs over limited periods, without explicitly reconstructing storage–elevation curves, long-term storage series or cross-border teleconnections with the terminal Lai Chau reservoir (Cường, 2025). Current applications also tend to provide only monthly water level–area information for specific modelling studies, rather than high-frequency,

[1]Thuyloi University
[2]Hanoi University of Natural Resources and Environment
[3]National Centre of Hydro–Meteorology Forecasting
[*] Corresponding author
Received 4th Dec. 2025
Accepted 20th Dec. 2025
Publication date 31st Dec. 2025

DEM-consistent area-elevation-volume relationships, fully automated Sentinel-1-based storage time series for the entire cascade, or a systematic diagnosis of cascade-scale regulation patterns and transboundary teleconnections (Tien Giang, Ba Huy, & Van Hai, 2025).

As a result, there is still no generic, open-data-based framework that can simultaneously (i) generate consistent F–Z–V curves and sub-monthly storage time series for all major reservoirs in the upper Da River and (ii) diagnose, in a systematic way, cascade-scale regulation patterns and teleconnections between Chinese reservoirs and the Lai Chau reservoir. This study addresses these gaps by developing a Sentinel-1- and DEM-based workflow on the Google Earth Engine platform to derive F–Z–V relationships, reconstruct reservoir storage dynamics, and analyse cascade behaviour and cross-border teleconnections in the upper Da River basin.

## 2. Material and methods

### *2.1. Study area and Data*

The Da River basin (20°40′–25°00′N; 100°22′–105°24′E) is oriented northwest–southeast, with a main channel length of about 667 km, of which roughly 383 km lie in China. The drainage area is ~52,900 km², with about 47% in China, 2% in Laos and 51% in Viet Nam; the Da River contributes around 37% of the total discharge of the Red River at Son Tay (Lê Bắc Huỳnh, 2003; Trương Vân Anh, 6/2017).

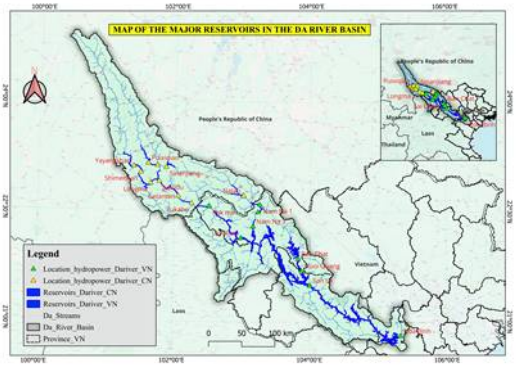


**Figure 1.** Map of the major reservoirs in the Da river basin

*Data used:* Reservoir polygons in Viet Nam were manually digitised in QGIS from high-resolution optical imagery, whereas Chinese reservoir outlines were taken from the published geospatial database of nearly 100,000 reservoirs in China (Song). These vector masks were combined with the 30 m NASADEM digital elevation model (NASA/JPL) to derive DEM-based area–elevation–volume (F–Z–V) curves, and with Sentinel-1 GRD IW imagery (10 m, VV/VH; Copernicus/ESA) and the JRC Global Surface Water occurrence product (European Commission) to map water surface area and constrain near-shore classification. Survey-based F–Z curves and in situ water-level records for Lai Chau and Huoi Quang were used for calibration and validation. All satellite datasets were accessed and processed within the Google Earth Engine environment.

### *2.2. Methods*

In this study we develop an end-to-end, fully satellite-based workflow on the Google Earth Engine platform to reconstruct reservoir area–elevation–volume (F–Z–V) relationships and storage dynamics for the upper Da River cascade. Reservoir polygons, NASADEM, Sentinel-1 GRD and JRC Global Surface Water are first combined to derive 1-m step F–Z–V curves using cleaned reservoir masks, trapezoidal integration and a vertical bias correction (zBias) constrained by available survey F–Z curves and in situ water levels. Sentinel-1 imagery is then pre-processed (orbit/polarisation selection, 7-day percentile compositing, 10-m terrain correction) and passed through a fast "OtsuSmart" classifier that applies shoreline ring histograms, percentile-based backup thresholds and JRC is used as an auxiliary dataset (AOI/QA), while thresholding relies on SAR backscatter, followed by morphological filtering to retain the main water patch. This yields 7-day water-surface area time series which are quality-controlled with a Hampel filter and mapped back to water level and storage via the DEM-derived F–Z–V curves, producing daily/7-day series of area, level and storage for each reservoir.

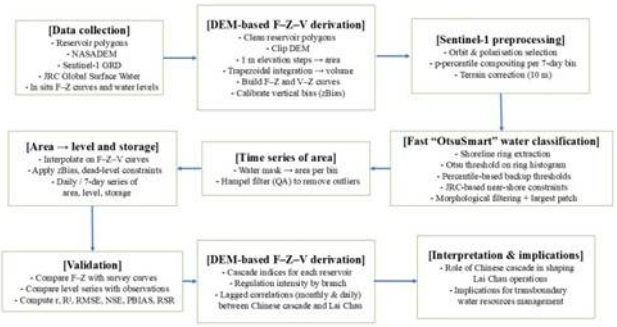


**Figure 2.** Study Flowchart

OtsuSmart retains the classical Otsu criterion for threshold selection, but improves robustness for narrow, canyon-type reservoirs by computing the histogram within a shoreline ring and fusing the ring-based Otsu threshold with percentile-based fallback thresholds (ring and AOI) using a median rule, followed by SAR-specific preprocessing (percentile compositing, radiometric normalization, speckle filtering) and postprocessing (morphological cleaning and largest-component retention).

The resulting F–Z–V products and time series are validated against independent survey curves and observed water levels, and then used to derive cascade indices, branch-wise regulation intensity and lagged correlations (monthly and daily) between the Chinese

reservoirs and Lai Chau. Compared with previous studies, the approach is novel in that it (i) generates DEM-consistent F–Z–V curves and sub-monthly storage time series for an entire transboundary cascade using only global open datasets, (ii) employs a generic, automated Sentinel-1 "OtsuSmart" classifier tailored to narrow, canyon-type reservoirs, and (iii) provides a quantitative, satellite-based diagnosis of cross-border regulation patterns and teleconnections that can be directly used to inform transboundary reservoir management.

## 3. Results and discussion

### *3.1. Construction of reservoir characteristic curves*

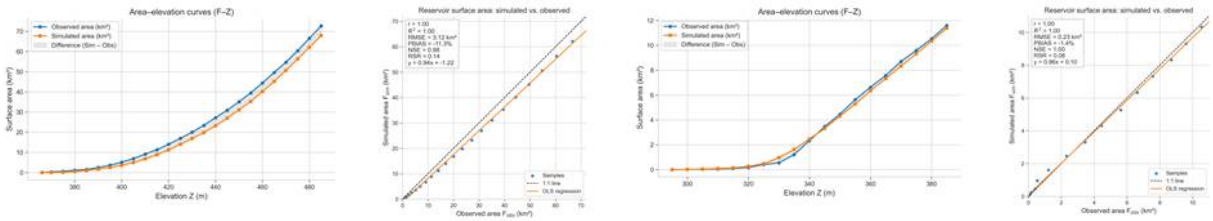


**Figure 3.** Comparison between calculated and observed of Lai Chau and Huoi Quang reservoirs

In this study, two reservoirs with contrasting size and morphology along the Da River were selected for validation: the large, multi-arm Lai Chau reservoir and the smaller, long and narrow Huoi Quang reservoir. For Lai Chau, the remote-sensing method reproduces the survey-based area–elevation (F–Z) curve with r = 1.00, $R^2$ = 1.00, RMSE = 1.86 km², NSE = 0.99, PBIAS ≈ –7.3% and RSR ≈ 0.10, indicating an almost perfect match with a moderate multiplicative underestimation that can be corrected by simple regression scaling. For Huoi Quang, performance is similarly high (r = 1.00, $R^2$ = 1.00, RMSE = 0.23 km², NSE ≈ 1.00, RSR = 0.06, PBIAS = –1.4%), with elevation-dependent errors remaining within about ±0.4 km² and no visible distortion of curve shape. Compared with a previous DEM-based study for Lai Chau (CC = 0.99, $R^2$ = 0.98, RMSE = 2.99 km², PBIAS = +6.74%, RSR = 0.27 (Cường, 2025), the present method achieves similar correlation but substantially lower RMSE and RSR, with a bias of comparable magnitude. These results show that the proposed approach can recover F–Z curves with near-perfect shape and small, mostly multiplicative biases across a wide range of reservoir geometries, providing a robust basis for deriving F–Z and subsequent elevation–storage (Z–V) relationships for data-scarce transboundary reservoirs in the upper Da River.

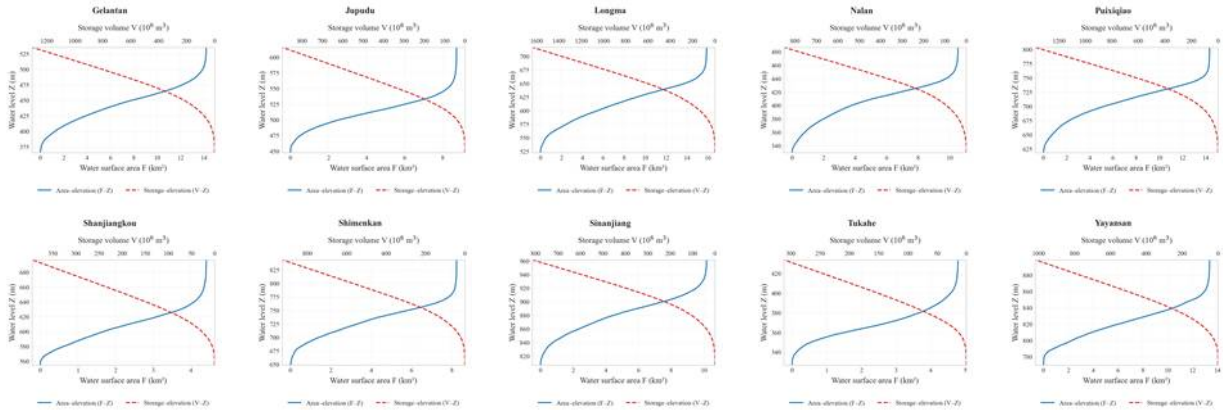


**Figure 4.** Characteristic curves of the Da river basin reservoirs (China)

### *3.2. Operation of the Chinese cascade and its influence on Lai Chau*

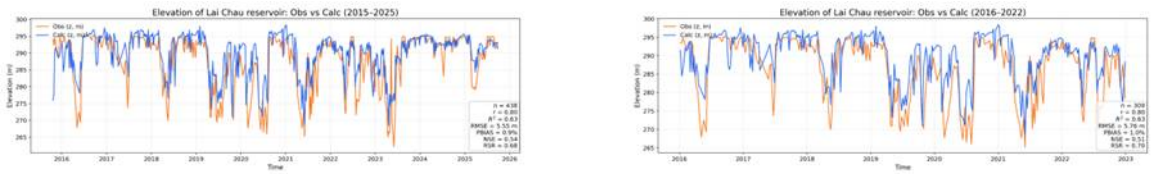


**Figure 5.** Comparison between calculated and observed water levels in the Lai Chau reservoir

In our experiment, the reconstructed water level at Lai Chau reproduces the observed series with r = 0.80, $R^2$ = 0.63, RMSE = 5.76 m, PBIAS ≈ –1.0 %, NSE = 0.51 and RSR = 0.70 for 2016–2022. For the extended period 2015–2025, the skill is very similar (r = 0.80, $R^2$ = 0.63, RMSE = 5.55 m, |PBIAS| ≈ 1 %, NSE = 0.54, RSR = 0.68), indicating stable performance. Tran Manh Cuong et al. (Cường, 2025) reported slightly higher correlation (CC = 0.87, $R^2$ = 0.76) but larger errors and poorer fit (PBIAS = –1.87 %, RMSE = 6.40 m, RSR = 1.06). According to RSR and NSE, our approach shifts the model from an unsatisfactory range (RSR > 1) to a satisfactory–good range (RSR ≈ 0.7, NSE ≈ 0.5) while keeping bias near zero, thus providing a more balanced and reliable reconstruction of Lai Chau water levels.

The reconstructed time series of water surface area, water level and storage reveal a strongly regulated regime across the upper Da River cascade during 2017–2024 (Figure 6). All reservoirs exhibit a coherent monsoon–dry-season cycle, with storage building up during the wet season and being released in the dry season, but the amplitude and timing of these cycles vary markedly with reservoir size, position in the cascade and operating objectives. Smaller upstream reservoirs show particularly strong year-to-year variability in wet-season filling levels, indicating closer tracking of inflow variability and more limited buffering capacity.

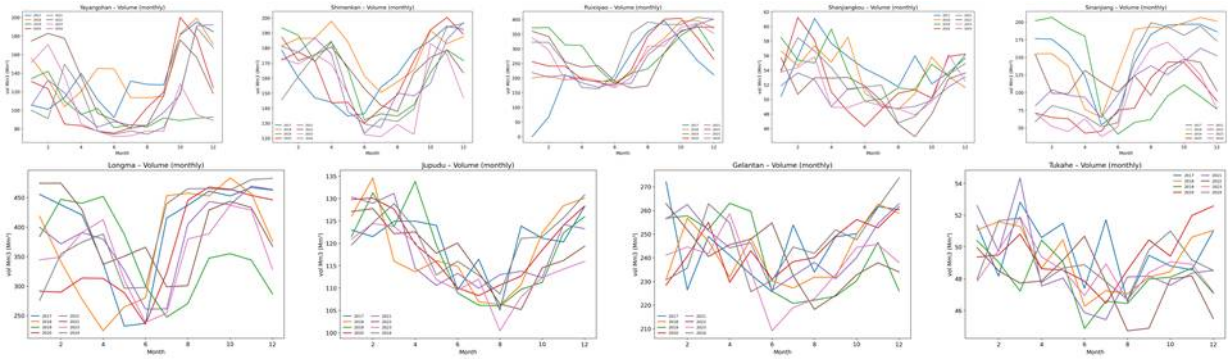


**Figure 6.** Changes in reservoir volume over the period 2017–2024

The joint analysis of area, level and storage highlights the added value of the F–Z–V framework. In deep, canyon-type reservoirs, surface-area changes are often modest while storage changes are large due to steep Z–V curves, so analyses based only on area would underestimate the degree of regulation-especially in the narrow, steep Chinese reaches of the Da River. By explicitly converting area time series into storage, the proposed method provides a more physically meaningful description of each reservoir's role within the cascade.

The cascade index (0–1) shows a strong annual cycle over 2017–2025, with typical values between 0.2 and 0.8 and occasional peaks near 0.9 when the cascade is almost full, while minima around 0.2 indicate strongly drawn-down conditions (Figure 7). The monthly climatology confirms lowest mean values in May–June (≈0.2–0.3) and highest in October–December (≈0.7–0.75), revealing a systematic shift from a low-storage, high-release regime in early monsoon months to a high-storage regime in late monsoon and early dry-season months.

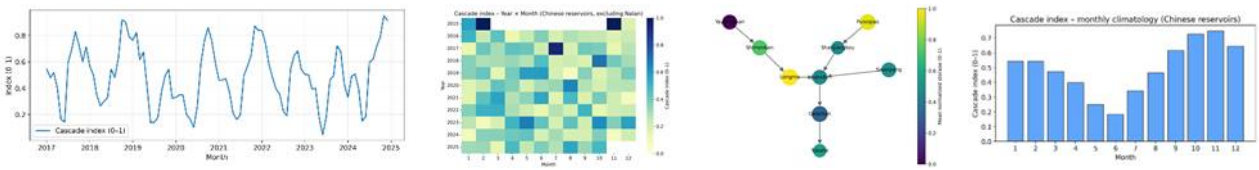


**Figure 7.** Cascade index patterns in Chinese reservoirs

In space, the indices distinguish upstream storage-type reservoirs-with high storage ratios and large seasonal cycles-from downstream reservoirs closer to the border, which have smaller relative cycles and higher spill fractions, consistent with mixed run-of-river and peaking operation. Timing metrics show that upstream reservoirs generally start releasing earlier, while downstream reservoirs delay drawdown, producing a staggered pattern of minimum storage levels along the cascade. This satellite-based framework compactly quantifies previously qualitative descriptions of Chinese reservoir operation and highlights where changes in management are likely to have the strongest downstream effects (Cường, 2025).

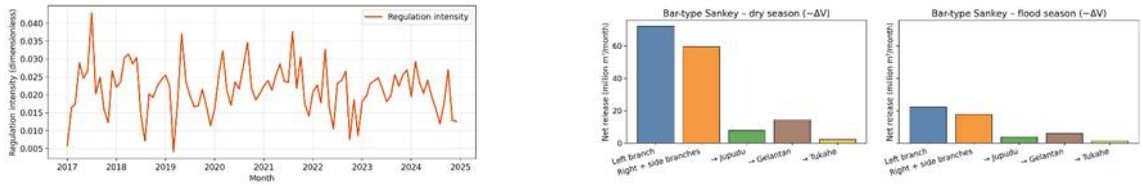


**Figure 8.** Regulation intensity and branch contributions

The regulation intensity index shows marked intra-annual and inter-annual variability over 2017–2024 (Figure 8a), with values ranging from about 0.01 to 0.04 and a median near 0.02. Most wet seasons display peaks of 0.025–0.035, while dry-season minima cluster around 0.012–0.015. Very strong regulation episodes with peaks above 0.035 occur in 2017, 2019 and 2022, whereas after 2022 the amplitude decreases and peaks rarely exceed 0.03, suggesting slightly more moderate regulation but no clear long-term trend.

The bar-type Sankey diagrams (Figure 8b) show that, in the dry season, net releases are dominated by the upstream branches (≈70 and ≈60 million m³ month⁻¹ for the left and right+side branches), while the main-stem reservoirs contribute smaller volumes (≈15, 10 and only a few million m³ month⁻¹ for Jupudu, Gelantan and Tukahe). In the flood season, all contributions decline sharply to about 20 and 10–12 million m³ month⁻¹ from the branches and 5, 2–3 and <1 million m³ month⁻¹ from the main-stem dams. Together, these results indicate that most regulation is achieved by storing water in the branches during the wet season and releasing it in the dry season, with the lower main-stem reservoirs mainly fine-tuning and redistributing flows. Consequently, dry-season support to Lai Chau depends primarily on how strongly the upstream branches are operated in storage mode, while the downstream trunk plays a secondary regulatory role.

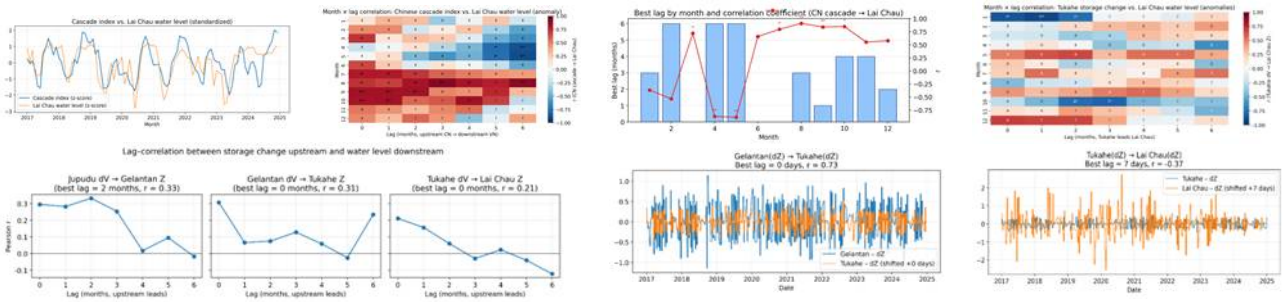


**Figure 9.** Storage and water level along the Jupudu-Gelantan-Tukahe-Lai Chau chain and Detailed Tukahe → Lai Chau relationship

The teleconnection analysis shows a strong but seasonally varying coupling between the Chinese cascade and the Lai Chau reservoir. The standardized cascade index and Lai Chau water level share a pronounced annual cycle, with upstream peaks and troughs occurring slightly earlier and with larger amplitude; month–lag correlations are predominantly positive during the main filling period, with best lags of 0–2 months and coefficients often above ~0.6, but weaken or become negative in some early-year months when local operation at Lai Chau partly offsets upstream changes.

Along the Jupudu–Gelantan–Tukahe–Lai Chau chain, normalized storage and level series remain coherent while variability attenuates downstream. Monthly lag–correlation curves indicate that storage changes at Jupudu lead Gelantan by about two months ($r \approx 0.33$), Gelantan and Tukahe are almost synchronous (lag 0 months, $r \approx 0.31$), and Tukahe retains a weaker yet positive influence on Lai Chau (lag 0 months, $r \approx 0.21$), with the cross-border link strongest at short lags during the monsoon. At the daily scale, Gelantan and Tukahe are tightly coupled (lag 0 days, $r \approx 0.73$), whereas Tukahe and Lai Chau display a moderate but significant negative correlation with a best lag of about seven days ($r \approx -0.37$), implying that rapid storage increases upstream are typically followed, about one week later, by drawdown at Lai Chau. Overall, the Chinese cascade exerts first-order control on the seasonal water-level regime at Lai Chau, while the Vietnamese terminal reservoir is actively used to buffer and counteract a substantial part of the sub-monthly variability imported from upstream.

## 4. Conclusions

A fully satellite-based workflow was implemented on Google Earth Engine to derive DEM-consistent F–Z–V curves and sub-monthly storage time series for all major reservoirs in the upper Da River cascade, using only open global datasets and minimal in situ information. Validation for Lai Chau and Huoi Quang shows that the method reproduces survey-based F–Z curves with near-perfect correlation ($r = 1.00$) and

small errors, and reconstructs Lai Chau water levels with r ≈ 0.80 and NSE ≈ 0.5, improving RMSE and RSR relative to previous DEM-based studies. Cascade and regulation indices quantify a systematic operating pattern in which reservoirs transition from a low-storage, high-release regime in early monsoon months to high-storage conditions in late monsoon and early dry seasons, with most net seasonal release provided by upstream branches rather than main-stem reservoirs. Teleconnection analyses at monthly and daily scales demonstrate that the Chinese cascade exerts first-order control on the seasonal water-level regime at Lai Chau, while the Vietnamese terminal reservoir is operated to buffer and counteract much of the high-frequency variability generated upstream. The proposed framework offers a transferable tool for diagnosing reservoir behaviour and cross-border regulation in other transboundary basins where detailed operational data are scarce, and can support future work on coupled modelling, scenario analysis and cooperative reservoir management.

**Acknowledgement**

We would like to thank the Project "Research and Development of a Remote Sensing and Artificial Intelligence–Based Monitoring Tool for Hydrological Characteristics, Surface Water Resources, and Land Cover to Support Forecasting and Early Warning of Hydrological Hazards in the Red River Basin." (Project Code: TNMT.2024.06.07) for its support in carrying out this study.

**Competing interests:** The authors declare that there is no conflict of interest regarding the publication of this article.

Link Code GEE: https://code.earthengine.google.com/29893c673a59102b0c840dfc0c820c2b

**References**

Condeça, J., Nascimento, J., & Barreiras, N. J. W. R. R. (2022). *Monitoring the storage volume of water reservoirs using Google Earth Engine*. 58(3), e2021WR030026.

Cường, T. M., et al. (2025). *Nghiên cứu giám sát hoạt động của các hồ chứa trên lưu vực sông Đà ngoài lãnh thổ Việt Nam từ dữ liệu vệ tinh và địa hình trên nền tảng Google Earth Engine.* Journal of Hydro-meteorology, 2(770), 84-96. doi:10.36335/vnjhm.2025(770).84-96

Du, T. L. T., Lee, H., Bui, D. D., Graham, L. P., Darby, S. D., Pechlivanidis, I. G., . . . Hwang, E. (2022). *Streamflow Prediction in Highly Regulated, Transboundary Watersheds Using Multi-Basin Modeling and Remote Sensing Imagery.* Water Resour Res, 58(3), e2021WR031191. doi:10.1029/2021WR031191

Giuliani, M., & Castelletti, A. (2013). *Assessing the value of cooperation and information exchange in large water resources systems by agent-based optimization.* Water Resources Research, 49(7), 3912-3926. doi:10.1002/wrcr.20287

He, D., Chen, X., Ji, X., Hu, J., Bao, A., Zhong, R., . . . Guli·Jiapaer. (2017). *International Rivers and Transboundary Environment and Resources*. In The Geographical Sciences During 1986-2015 (pp. 469-480).

Kumar Biswas, N., & Hossain, F. J. J. o. H. (2022). *A multidecadal analysis of reservoir storage change in developing regions*. 23(1), 71-85.

Lê Bắc Huỳnh, L. T. V. H. (2003). *Hoàn thiện mô hình tính toán và dự báo dòng chảy sông Đà phục vụ điều hành hồ Hòa Bình.* Tạp chí Khí tượng Thủy văn, 508.

Oliver Olsson, M. G., Kai Wegerich, Melanie Bauer. (2010). *Identification of the effective water availability from streamflows in the Zerafshan river basin, Central Asia.* Journal of Hydrology, 390, 190–197. doi:10.1016/j.jhydrol.2010.06.042

Pham-Duc, B., Frappart, F., Tran-Anh, Q., Si, S. T., Phan, H., Quoc, S. N., . . . Viet, B. D. (2022). *Monitoring Lake Volume Variation from Space Using Satellite Observations-A Case Study in Thac Mo Reservoir (Vietnam).* Remote Sensing, 14(16). doi:10.3390/rs14164023

Song, C., et al. *A comprehensive geospatial database of nearly 100 000 reservoirs in China.* Earth System Science Data, 14, 4017-4034. doi:10.5194/essd-14-4017-202210.5281/zenodo.6984619

Tien Giang, N., Ba Huy, D., & Van Hai, K. (2025). *Develop Operation Rules for Reservoirs in the Upper Da River Basin Using Multi-source Remote Sensing Data.* VNU Journal of Science: Earth and Environmental Sciences, 41(1S). doi:10.25073/2588-1094/vnuees.5389

Trương Vân Anh, N. T. H., Đặng Quốc Khánh. (6/2017). *Nghiên cứu đánh giá lượng dòng chảy sông Đà từ Trung Quốc vào Việt Nam phục vụ cho bài toán quy hoạch và quản lý tài nguyên nước lưu vực sông Đà.* Tạp chí Khí tượng Thủy văn.

Vu, D. T., Dang, T. D., Galelli, S., & Hossain, F. (2022). *Satellite observations reveal 13 years of reservoir filling strategies, operating rules, and hydrological alterations in the Upper Mekong River basin.* Hydrology and Earth System Sciences, 26(9), 2345-2364. doi:10.5194/hess-26-2345-2022